Title

Identification and characterization of VpsR and VpsT binding sites in Vibrio cholerae.

Journal

Journal of Bacteriology, 197(7)

Authors

Zamorano-Sánchez, David

Fong, Jiunn

Kilic, Sefa

et al.

Publication Date

2015-04-01

DOI

10.1128/JB.02439-14

Peer reviewed

JB Journals.ASM.org

Identification and Characterization of VpsR and VpsT Binding Sites in *Vibrio cholerae*

David Zamorano-Sánchez,[a] Jiunn C. N. Fong,[a] Sefa Kilic,[b] Ivan Erill,[b] Fitnat H. Yildiz[a]

Department of Microbiology and Environmental Toxicology, University of California, Santa Cruz, Santa Cruz, California, USA[a]; Department of Biological Sciences, University of Maryland Baltimore County (UMBC), Baltimore, Maryland, USA[b]

ABSTRACT

The ability to form biofilms is critical for environmental survival and transmission of *Vibrio cholerae*, a facultative human pathogen responsible for the disease cholera. Biofilm formation is controlled by several transcriptional regulators and alternative sigma factors. In this study, we report that the two main positive regulators of biofilm formation, VpsR and VpsT, bind to nonoverlapping target sequences in the regulatory region of *vpsL in vitro*. VpsR binds to a proximal site (the R1 box) as well as a distal site (the R2 box) with respect to the transcriptional start site identified upstream of *vpsL*. The VpsT binding site (the T box) is located between the R1 and R2 boxes. While mutations in the T and R boxes resulted in a decrease in *vpsL* expression, deletion of the T and R2 boxes resulted in an increase in *vpsL* expression. Analysis of the role of H-NS in *vpsL* expression revealed that deletion of *hns* resulted in enhanced *vpsL* expression. The level of *vpsL* expression was higher in an *hns vpsT* double mutant than in the parental strain but lower than that in an *hns* mutant. *In silico* analysis of the regulatory regions of the VpsR and VpsT targets resulted in the identification of conserved recognition motifs for VpsR and VpsT and revealed that operons involved in biofilm formation and *vpsT* are coregulated by VpsR and VpsT. Furthermore, a comparative genomics analysis revealed substantial variability in the promoter region of the *vpsT* and *vpsL* genes among extant *V. cholerae* isolates, suggesting that regulation of biofilm formation is under active selection.

IMPORTANCE

***Vibrio cholerae* causes cholera and is a natural inhabitant of aquatic environments. One critical factor that is important for environmental survival and transmission of *V. cholerae* is the microbe's ability to form biofilms, which are surface-associated communities encased in a matrix composed of the exopolysaccharide VPS (*Vibrio* polysaccharide), proteins, and nucleic acids. Two proteins, VpsR and VpsT, positively regulate VPS production and biofilm formation. We characterized the structural features of the promoter of the *vpsL* gene, determined the target sequences recognized by VpsT and VpsR, and analyzed their distribution and conservation patterns in multiple *V. cholerae* isolates. This work fills a fundamental gap in our understanding of the regulatory mechanisms employed by the master regulators VpsR and VpsT in controlling biofilm matrix production.**

Biofilms are microbial communities composed of aggregated microorganisms and an exopolymeric matrix typically made up of exopolysaccharides, proteins, and nucleic acids. These microbial structures are prevalent in nature and are often found attached to abiotic or biotic surfaces (1). *Vibrio cholerae*, a human pathogen that can colonize the human intestine and cause the diarrheal disease cholera, is an autochthonous member of estuarine environments (2, 3). In aquatic environments, *V. cholerae* can form biofilms on various surfaces, including phytoplankton, zooplankton, and sediments (4–8). The ability of this pathogen to disseminate and persist in aquatic reservoirs and to be transmitted to a new human host is significantly influenced by its ability to form biofilms (5, 7, 9–11).

The *V. cholerae* extracellular matrix is composed of a glycoconjugate termed VPS (*Vibrio* polysaccharide) (12, 13) and three major matrix proteins, RbmA, RbmC, and Bap1, involved in cell-cell and cell-surface adhesion (14–18). The biosynthesis of VPS depends on the presence of two operons, *vps*-I (*vpsU* to *vpsK* loci) and *vps*-II (*vpsL* to *vpsQ* loci) (12, 19). The *vps*-I and *vps*-II operons are in close genomic proximity and are separated by an 8.3-kb region harboring *rbm* genes that encode matrix proteins (14, 15). The other major matrix protein is encoded by the *bap1* gene, located elsewhere in *V. cholerae* chromosome I (15, 16). Transcription of the genes encoding VPS and matrix proteins is increased when intracellular levels of the second messenger, cyclic-di-GMP (c-di-GMP), are elevated (20–22). Two transcriptional regulators, VpsR and VpsT, positively regulate biofilm gene expression (23, 24). These two regulators share structural characteristics with the response regulators of two-component systems and have been shown to bind c-di-GMP *in vitro* (25, 26). The levels of c-di-GMP affect the ability of VpsR to activate the expression of *vpsT* and *aphA* (encoding a transcriptional activator of virulence genes) (26). However, contrary to what has been observed for VpsT, VpsR does not require the presence of c-di-GMP to bind to the regulatory region of its targets *in vitro* (26). The crystal structure of

Received 25 October 2014 **Accepted** 21 January 2015

Accepted manuscript posted online 26 January 2015

Citation Zamorano-Sánchez D, Fong JCN, Kilic S, Erill I, Yildiz FH. 2015. Identification and characterization of VpsR and VpsT binding sites in *Vibrio cholerae*. J Bacteriol 197:1221–1235. doi:10.1128/JB.02439-14.

Editor: G. A. O'Toole

Address correspondence to Fitnat H. Yildiz, fyildiz@ucsc.edu.

Supplemental material for this article may be found at http://dx.doi.org/10.1128/JB.02439-14.

doi:10.1128/JB.02439-14

the VpsT/c-di-GMP complex revealed the VpsT c-di-GMP binding motif is 4 residues long [W(F/L/M)(T/S)R] and established that these residues are important for the activity of VpsT both *in vivo* and *in vitro* (25). These studies also showed that VpsT forms a dimer and that the c-di-GMP-dependent interaction between two VpsT monomers is sufficient and necessary for DNA recognition and transcriptional regulation.

Genes regulated by VpsR and VpsT were identified by transcriptional profiling (27, 28). The genes that exhibit the strongest dependence on VpsR and VpsT for their expression belong to the *vps* and *rbm* clusters. Other genes regulated by VpsR and VpsT include genes of the extracellular protein secretion (ESP) general secretion system and genes for nucleotide biosynthesis, sugar transport, and c-di-GMP metabolism, as well as several genes encoding hypothetical proteins of unknown function and genes annotated as putative transcriptional regulators (27, 28). Analysis of upstream regulatory regions of VpsR-regulated genes resulted in the identification of a conserved motif predicted to be the VpsR binding site (27). Notably, VpsR was shown to bind to a region containing the predicted VpsR binding motif located upstream of *aphA*; the VpsR recognition site overlaps the recognition site of HapR (29). Recent studies showed that VpsT can bind to the regulatory region of *vpsL* and *rpoS* in a c-di-GMP-dependent manner (25, 30). Two inverted repeats were found in the VpsT recognition site at the *rpoS* promoter, yet this motif was not found in the regulatory region of *vps* genes (30).

VpsR and VpsT control each other's expression, making it difficult to define which targets are specific for each regulator. Regulators such as HapR and H-NS have been shown to repress biofilm formation through direct regulation of VpsT, the *vps* clusters, and genes involved in c-di-GMP metabolism (31, 32). The global regulator cyclic AMP receptor protein has also been shown to repress biofilm formation and affects the expression of *vpsR*, *vpsT*, *hapR*, and the *vps* and *rbm* clusters, along with several other genes (33–35). A better understanding of the molecular mechanisms employed by VpsR and VpsT to control gene expression is instrumental in determining how the interplay between several activators and repressors controls the development of *V. cholerae* biofilms.

To gain an insight into the molecular basis of regulation employed by VpsR and VpsT in controlling the expression of matrix genes and other potential targets, we focused on the regulatory region of *vpsL*, the first gene of the *vps*-II operon. In strains lacking *vpsR*, expression of the *vpsL* gene is abolished, while disruption of *vpsT* reduces the expression of *vpsL* and matrix protein genes as well as the formation of the typical three-dimensional biofilm structure. It has previously been shown that VpsT can bind to the regulatory region of *vpsL* (25), and there is strong evidence to suggest that VpsR is directly involved in the transcription of *vpsL* (27). However, the need for both regulators to be present in the cell to achieve maximal levels of expression is poorly understood. Here we report that (i) VpsR and VpsT recognize nonoverlapping target sequences, (ii) the identified target sequences are necessary for optimal expression, and (iii) the distal VpsR binding site and the VpsT binding site are dispensable in the absence of H-NS. Using an *in silico* approach, we define potential target sequences recognized by VpsT and VpsR and analyze their distribution and conservation patterns in multiple *V. cholerae* isolates. This work fills a fundamental gap in our understanding of the regulatory mechanisms employed by the master regulators VpsR and VpsT in controlling biofilm matrix production. It also allows us to propose new venues to evaluate the connection between regulatory subnetworks involved in biofilm development.

MATERIALS AND METHODS

Strains and growth conditions. The *Escherichia coli* and *V. cholerae* strains as well as the plasmids used in this study are described in Table 1. *E. coli* and *V. cholerae* strains were grown in Luria-Bertani broth (LB) (1% tryptone, 0.5% yeast extract, 1% NaCl), pH 7.5, at 37°C and 30°C, respectively. LB agar medium contained 1.5% (wt/vol) granulated agar (Difco). The following antibiotics were added at the indicated concentrations: ampicillin at 100 μg/ml and chloramphenicol at 20 μg/ml for *E. coli* and chloramphenicol at 5 μg/ml, rifampin at 100 μg/ml, and kanamycin at 50 μg/ml for *V. cholerae*.

Recombinant DNA techniques. DNA manipulations were carried out by standard molecular techniques. The primer sequences used in this work are shown in Table S1 in the supplemental material. Primers were designed using the web interface Primer3Plus (36). Unlabeled primers were purchased from Bioneer Corporation (Alameda, CA) and Integrated DNA Technologies (Coralville, IA). Primers fluorescently labeled at the 5′ end were purchased from Bioneer Corporation (Cy3) and Applied Biosystems (Grand Island, NY) (6-carboxyfluorescein [FAM] and VIC). PCR amplification was performed using the Phusion High-Fidelity PCR master mix (New England BioLabs, Ipswich, MA). PCR products were purified using a Wizard SV gel and PCR cleanup system (Promega, Madison, WI). Plasmid isolation was performed using a PureYield plasmid miniprep system (Promega, Madison, WI). Overlap extension PCR was performed in three steps. PCR products A and B (or A, C, and D) containing 3′ and 5′ overlapping overhangs were amplified using standard thermal cycling parameters. These two PCR products were annealed together and extended using a cycling regime of 10 cycles of 92°C for 40 s, 50°C for 40 s, and 72°C for 45 s. The product of this PCR was used as the template for amplification using the outermost primers containing appropriate restriction sites for cloning into the destination vector. Restriction and DNA modification enzymes were purchased from New England BioLabs (NEB; Ipswich, MA). All plasmid constructs were sequenced at the University of California, Berkeley, DNA sequencing facility to check for the fidelity of amplification.

RNA isolation. Total RNA was isolated from *V. cholerae* cells grown aerobically to mid-exponential phase (optical density at 600 nm [OD_{600}] = 0.3 to 0.4) in LB medium at 30°C. Briefly, overnight-grown *V. cholerae* cultures were diluted 1:200 in fresh LB medium and were grown aerobically at 30°C with shaking at 200 rpm to an OD_{600} of 0.3 to 0.4. The cultures were reinoculated (1:200) into fresh LB medium until the OD_{600} reached 0.3 to 0.4. Aliquots (2 ml) of the cultures were collected and centrifuged for 2 min at room temperature. Cell pellets were immediately resuspended in 1 ml of TRIzol reagent (Invitrogen, Grand Island, NY) and stored at −70°C. Total RNA was isolated according to the manufacturer's instructions. To remove contaminating DNA, total RNA was incubated with a Turbo DNA-free kit (Thermo Scientific, Grand Island, NY) and concentrated using an Isolate II RNA micro-cleanup kit (Bioline, Taunton, MA).

Primer extension. The transcriptional start site (TSS) of *vpsL* was determined by primer extension using a reverse primer conjugated with the FAM fluorophore (primer MSACE_*vpsL*_RvFAM) (see Table S1 in the supplemental material). Isolation of RNA from two independent samples of strains FY_Vc_9543 and FY_Vc_9544 was performed as described above. Total RNA (10 to 12 μg) was used as the template for the primer extension reaction in a final volume of 30 μl using a SuperScript III first-strand synthesis system (Thermo Scientific, Grand Island, NY) following the manufacturer's instructions. To hydrolyze the RNA, 3 μl of 1 N NaOH and 0.6 μl of 0.5 M EDTA were added. The mixture was incubated at 65°C for 10 min. HEPES, pH 7.0 (33.6 μl), was added to neutralize the solution. The primer extension products were purified and concentrated using a MinElute PCR purification kit (Qiagen, Valencia, CA). Automated fluo-

TABLE 1 Strains and plasmids used in this study

Strain or plasmid	Relevant properties[a]	Source or reference
Strains		
E. coli strains		
DH5α	F′ *endA1 hsdR17 supE44 thi-1 recA1 gyrA96 relA1* Δ(*argF-lacZYA*)*U169* ϕ80d*lac*ΔM15	Promega
CC118 (λ *pir*)	Δ(*ara-leu*) *araD* Δ*lacX74 galE galK phoA20 thi-1 rpsE rpoB argE*(Am) *recA1* λ *pir*	58
S17-1 (λ *pir*)	Tp^r Sm^r *recA thi pro hsdR17*(r_K^- m_K^+) *RP4*::*2-Tc*::Mu Km Tn*7* λ *pir*	59
BL21(DE3)	F^- *ompT hsdS*$_B$(r_B^- m_B^-) *gal dcm* (DE3)	Invitrogen
V. cholerae strains		
FY_Vc_2	O1 El Tor A1552, rugose variant, Rif^r	23
FY_Vc_5	Fy_Vc_2 Δ*vpsT* Rif^r	24
FY_Vc_6	Fy_Vc_2 Δ*vpsR* Rif^r	24
FY_Vc_9543	FY_Vc_2/pFY_3406 Rif^r Cm^r	This study
FY_Vc_9544	FY_Vc_6/pFY_3406 Rif^r Cm^r	This study
FY_Vc_9545	FY_Vc_2/pFY_3407 Rif^r Cm^r	This study
FY_Vc_9546	FY_Vc_2/pFY_3408 Rif^r Cm^r	This study
FY_Vc_9547	FY_Vc_2/pFY_3409 Rif^r Cm^r	This study
FY_Vc_9548	FY_Vc_2/pFY_3410 Rif^r Cm^r	This study
FY_Vc_9549	FY_Vc_2/pFY_3411 Rif^r Cm^r	This study
FY_Vc_9550	FY_Vc_2/pFY_3412 Rif^r Cm^r	This study
FY_Vc_9551	FY_Vc_2/pFY_3413 Rif^r Cm^r	This study
FY_Vc_9552	FY_Vc_2/pFY_3414 Rif^r Cm^r	This study
FY_Vc_9553	FY_Vc_2/pFY_3415 Rif^r Cm^r	This study
FY_Vc_9554	FY_Vc_2/pFY_3416 Rif^r Cm^r	This study
FY_Vc_9912	FY_Vc_2/pFY_3493 Rif^r Cm^r	This study
FY_Vc_9556	Fy_Vc_2 Δ*hns* Rif^r	This study
FY_Vc_9557	FY_Vc_9556/pFY_3406 Rif^r Cm^r	This study
FY_Vc_9558	FY_Vc_9556/pFY_3407 Rif^r Cm^r	This study
FY_Vc_9559	FY_Vc_9556/pFY_3408 Rif^r Cm^r	This study
FY_Vc_9560	FY_Vc_9556/pFY_3409 Rif^r Cm^r	This study
FY_Vc_9561	FY_Vc_9556/pFY_3410 Rif^r Cm^r	This study
FY_Vc_9913	FY_Vc_9556/pFY_3416 Rif^r Cm^r	This study
FY_Vc_9914	FY_Vc_5/pFY_3406 Rif^r Cm^r	This study
FY_Vc_9915	FY_Vc_5 Δ*hns*-FRT-Kan^r-FRT Rif^r	This study
FY_Vc_9916	FY_Vc_9915/pFY_3406 Rif^r Kan^r Cm^r	This study
Plasmids		
pMAL-c5x	IPTG-inducible expression vector with N-terminal MBP, Ap^r	NEB
pFY_1471	pMAL-c5x-*vpsT* Ap^r	This study
pFY_1472	pMAL-c5x-*vpsR* Ap^r	This study
pBBRlux	*luxCDABE*-based promoter fusion vector, Cm^r	60
pFY_3406	pBBRlux *vpsL* promoter, Cm^r (−607, +158)	This study
pFY_3407	pBBRlux *vpsL* promoter with mutated R1 box, Cm^r (−607, +158)	This study
pFY_3408	pBBRlux *vpsL* promoter with mutated T box, Cm^r (−607, +158)	This study
pFY_3409	pBBRlux *vpsL* promoter with mutated R2a box, Cm^r (−607, +158)	This study
pFY_3410	pBBRlux *vpsL* promoter with mutated R2b box, Cm^r (−607, +158)	This study
pFY_3411	pBBRlux *vpsL* promoter, Cm^r (−432, +158)	This study
pFY_3412	pBBRlux *vpsL* promoter, Cm^r (−379, +158)	This study
pFY_3413	pBBRlux *vpsL* promoter, Cm^r (−300, +158)	This study
pFY_3414	pBBRlux *vpsL* promoter, Cm^r (−272, +158)	This study
pFY_3415	pBBRlux *vpsL* promoter, Cm^r (−351, +158)	This study
pFY_3416	pBBRlux *vpsL* promoter, Cm^r (−250, +158)	This study
pFY_3493	pBBRlux *vpsL* promoter, Cm^r (−96, +158)	This study
pGP704-*sacB*28	pGP704 derivative, *mob-oriT sacB* Ap^r	G. Schoolnik
pFY_3418	pGP704-*sacB*28-Δ*hns* Ap^r	This study
pBR-FRT-Kan^r-FRT	pBR322 backbone	61

[a] Numbers in parentheses indicate the nucleotide positions of the cloned *vpsL* regulatory regions with respect to the translation start site.

rescent DNA analysis, alignment of the electropherograms, and signal normalization were done at the Plant-Microbe Genomic Facility at Ohio State University as previously reported (37) using the primers listed in Table S1 in the supplemental material and an unlabeled DNA template.

Purification of MBP-VpsR and MBP-VpsT. Plasmids pFY_1472 and pFY_1471 were used to overproduce VpsR and VpsT recombinant proteins, respectively, with a maltose binding protein (MBP) fused to the amino terminus (MBP-VpsR and MBP-VpsT) in *E. coli* BL21. Cells were

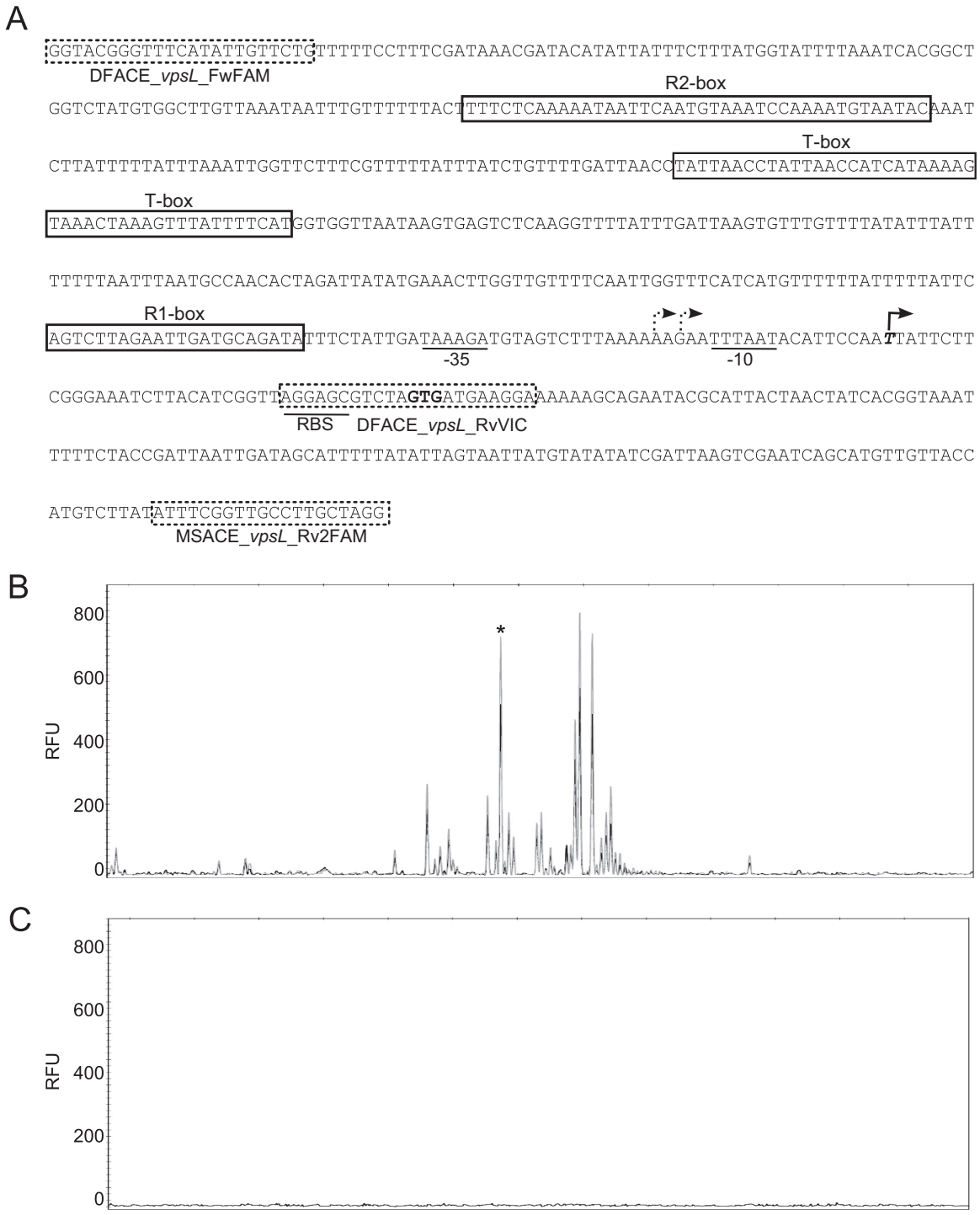

FIG 1 Characterization of *vpsL* promoter. (A) Sequence analysis of the regulatory region of *vpsL*. Putative promoter elements are underlined, and the *vpsL* start codon is in bold. The primary TSS is indicated with a solid arrow, and the corresponding nucleotide is in bold and italicized. Alternative TSSs are indicated with dotted arrows. The VpsT and VpsR protection sites are boxed. Oligonucleotides used for primer extension and DNase footprinting are boxed with dotted lines. (B, C) Electropherograms from primer extension products obtained with a fluorescently labeled primer (MSACE_*vpsL*_Rv2FAM). *x* axes represent values in base pairs. RFU, relative fluorescence units. (B) Superimposed electropherograms obtained from two independent primer extension experiments. The defined TSS is marked with an asterisk. (C) Electropherogram showing a lack of primer extension products when total RNA from a Δ*vpsR* strain was used as the template.

grown at 37°C with shaking (200 rpm) in 1 liter of rich medium (10 g tryptone, 5 g yeast extract, 5 g NaCl, 2 g of glucose per liter) supplemented with ampicillin (100 μg/μl) until the OD_{600} reached 0.5 for cells overexpressing MBP-VpsT or 0.2 for cells overexpressing MBP-VpsR. IPTG (isopropyl-β-D-thiogalactopyranoside) was added to a final concentration of 0.3 μM. Cells harboring pFY_1471 were further incubated for 4 h at 30°C with shaking (200 rpm), and cells harboring pFY_1472 were incubated overnight at 20°C with shaking (200 rpm). Cells were harvested

by centrifugation, resuspended in column buffer (20 mM Tris, pH 7.4, 1 mM EDTA, 200 mM NaCl), and lysed by sonication. The soluble fraction was separated by centrifugation at 20,000 × *g* and 4°C for 20 min. Proteins were purified using amylose resin (NEB, Ipswich, MA) following the manufacturer's instructions. Briefly, the protein extract (soluble fraction) was passed through an equilibrated gravity column packed with amylose resin. The resin was washed twice with column buffer (10 column volumes), and then the protein was eluted in several fractions by the addition of column buffer supplemented with 10 mM maltose. Samples from each step of the purification procedure were visualized in an SDS-polyacrylamide gel stained with Coomassie blue. The protein concentration was determined using a bicinchoninic acid protein assay kit (Thermo Scientific) and bovine serum albumin (BSA) as the standard.

DNase I footprinting. The DNase I footprinting experiments were performed using a probe labeled with the FAM fluorophore on the 5′ end and the VIC fluorophore on the 3′ end, followed by analysis with an automated fluorescent DNA analyzer to resolve the digested products, as reported previously (38). A forward primer conjugated with the FAM and a reverse primer conjugated with VIC were used to amplify a product that encompasses the *vpsL* intergenic region from positions −511 to +11 with respect to the start codon (522 bp). The PCR product was purified using the Wizard SV gel and PCR cleanup system (Promega, Madison, WI).

MBP-VpsT or MBP-VpsR (1 μM) was incubated for 10 min at room temperature in a binding buffer containing 100 mM Tris-HCl, pH 7.4, 100 mM KCl, 10 mM $MgCl_2$, 2 mM dithiothreitol, 10% glycerol, and 0.5 μg/μl of BSA. In the experiment involving the regulator VpsT, 50 μM c-di-GMP was also added to the binding reaction mixture. The fluorescently labeled probe (40 nM for the VpsR binding reaction or 10 nM for the VpsT binding reaction) was added to the binding reaction mixtures (final volume, 10 μl), and the mixtures were incubated for 30 min at room temperature. The negative control of the experiment was a binding reaction mixture lacking either VpsR or VpsT. The binding reaction mixtures and the negative control were used as the substrate in DNase I digestion reactions. DNase I (0.03 U; NEB, Ipswich, MA) was added, and the samples were incubated for 5 min at room temperature. To stop the reaction, the samples were heated to 75°C for 10 min. The digested fragments were purified using a MinElute PCR purification kit (Qiagen, Valencia, CA). The digested fragments were resolved using an automated fluorescent DNA analysis instrument (Applied Biosystems 3730 DNA analyzer) as described previously (38). Automated fluorescent DNA analysis, alignment of the electropherograms, signal normalization, and differential analysis of the DNase I footprinting results among the experimental samples and the negative control were done at the Plant-Microbe Genomic Facility at Ohio State University as reported previously (38, 39). The primers used in the DNase I footprinting experiments are listed in Table S1 in the supplemental material. DNA templates were generated with unlabeled primers.

EMSAs. Eight different probes labeled with either Cy3 or FAM were used for electrophoretic mobility shift assays (EMSAs). The primers and templates used to amplify each probe are listed in Table S1 in the supplemental material. The R2-T-R1 probe (522 bp) encompasses the region from positions −511 to +11 with respect to the translational start site of *vpsL*. The R1 probe (270 bp) encompasses the region from positions −250 to +11. The mutated R1 probe (270 bp) is similar to the R1 probe but has transversion mutations in the R1 box (mutations are indicated in Fig. 3 and 4). The R2 probe encompasses the region from positions −511 to −309. The mutated R2a probe is similar to the R2a probe but has transversion mutations (mutations are indicated in Fig. 3 and 4). The *tcpP* probe encompasses the region from positions −180 to +28 with respect to the start codon. This probe was used as a negative control. Each probe was purified from agarose gels using the Wizard SV gel and PCR cleanup system (Promega, Madison, WI), and the concentration was determined using a NanoDrop spectrophotometer (Thermo Scientific, Grand Island, NY).

The reaction mixture for the binding of MBP-VpsR or MBP-VpsT with target DNA was prepared as follows. Each probe (final concentration, 10 nM) and the protein (800 nM for VpsR, 300 nM for VpsT) were combined in a binding buffer containing 100 mM Tris-HCl (pH 7.4), 100 mM KCl, 10 mM $MgCl_2$, 10% glycerol, 2 mM dithiothreitol, 0.5 μg poly(dI-dC), and 0.5 μg/μl of BSA in a final volume of 10 μl. When noted,

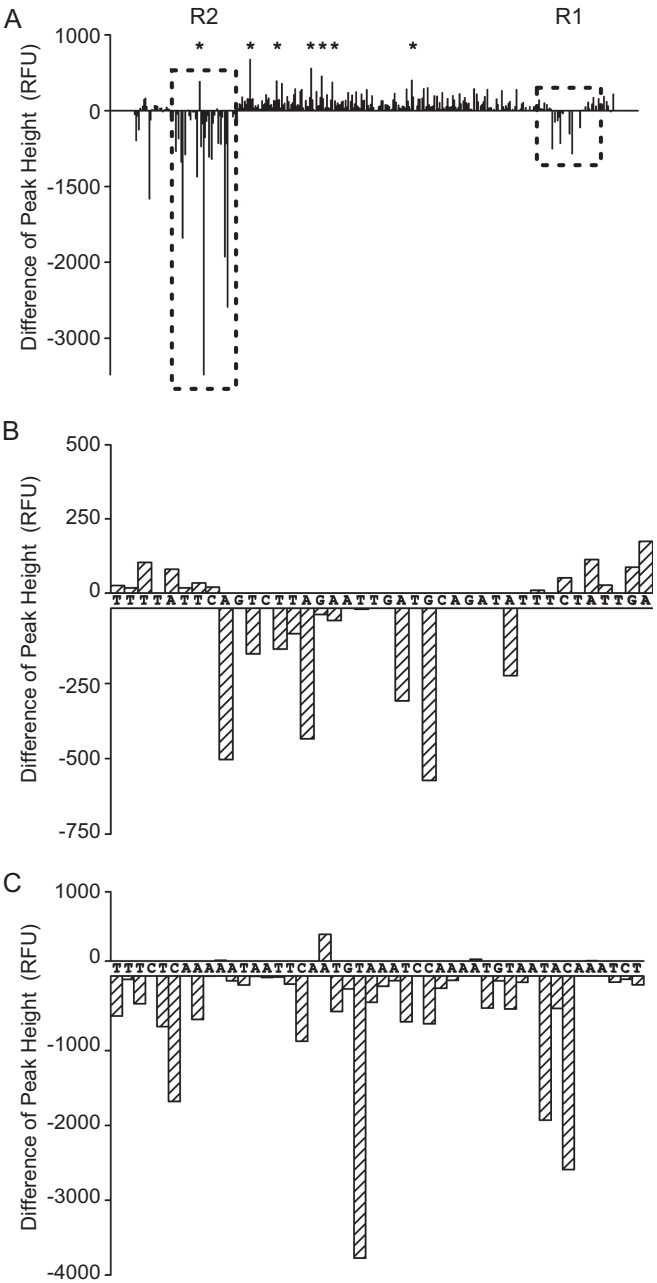

FIG 2 DNase I footprinting analysis of VpsR-protected regions. (A) Pattern of protection and hypersensitivity obtained with a fluorescently labeled probe (FAM) encompassing the *vpsL* regulatory region (positions −511 to +11). The difference in normalized peak height (in relative fluorescent units [RFU]) between the electropherograms for the experimental sample (VpsR-*vpsL*) and the negative control (BSA-*vpsL*) is plotted as a histogram. Negative peak heights represent protection, while positive peak heights are indicative of hypersensitivity. Potential hypersensitive sites (>300 RFUs) are marked with asterisks. (B, C) Two protection sites are observed in the presence of VpsR: the proximal R1 box and the distal R2 box. Nucleotide sequences for the R1 (B) and R2 (C) protected regions are shown.

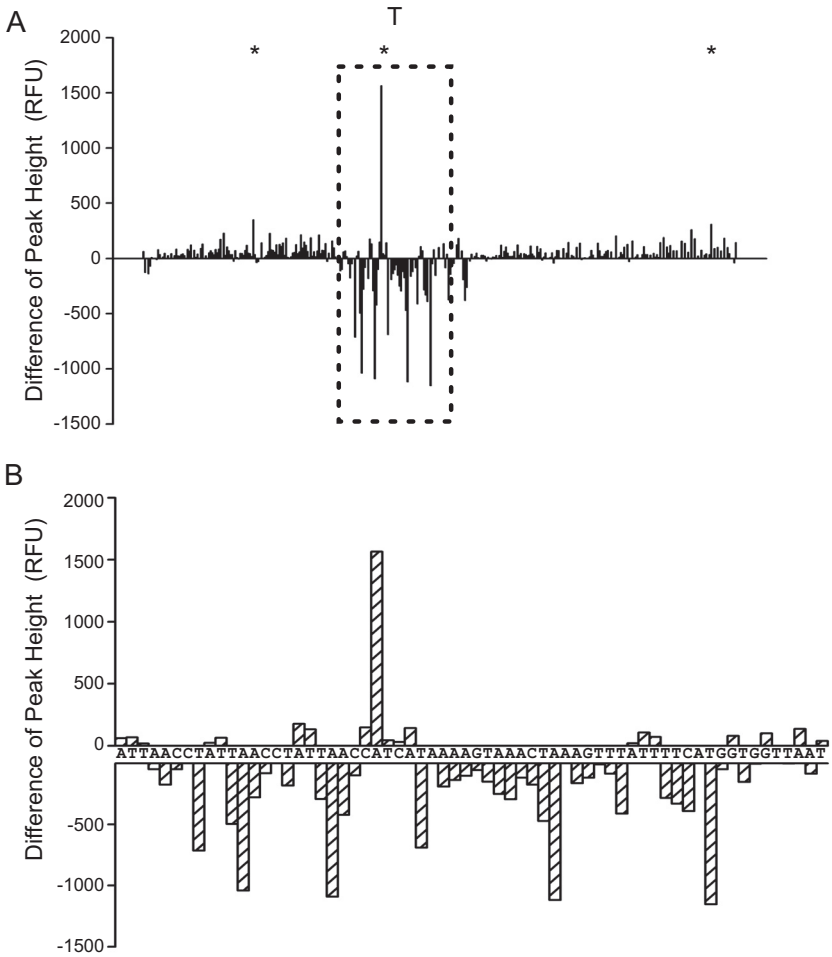

FIG 3 DNase I footprinting analysis of VpsT-protected region. (A) Pattern of protection and hypersensitivity obtained with a fluorescently labeled (FAM) probe encompassing the *vpsL* regulatory region (positions −511 to +11). The difference in normalized peak height (in relative fluorescent units [RFU]) between the electropherograms for the experimental sample (VpsT-*vpsL*) and the negative control (BSA-*vpsL*) is plotted as a histogram. Negative peak heights represent protection, while positive peak heights are indicative of hypersensitivity. Potential hypersensitive sites (>300 RFUs) are marked with asterisks. (B) The nucleotide sequence of the protected region is shown.

c-di-GMP was added to a final concentration of 50 μM. The binding reaction mixtures were incubated for 30 min at room temperature and then loaded into a native prerun 5% polyacrylamide (acrylamide-bisacrylamide ratio, 37.5:1)–1× Tris-borate-EDTA (TBE) gel and run at 4°C in 0.5× TBE buffer (Bio-Rad, Hercules, CA) for 30 min at 150 V. DNA migration was visualized using a Chemidoc MP imaging system (Bio-Rad, Hercules, CA).

Construction of transcriptional fusions. Transcriptional fusions with different fragments of the regulatory region of *vpsL* (pFY_3406 through pFY_3416 and pFY_3493) were generated with the primers listed in Table S1 in the supplemental material. PCR products were purified and digested with NheI and BamHI to clone directionally into the promoterless plasmid pBBRlux linearized with SpeI and BamHI. Transversion mutations in the R and T boxes were introduced with the primers listed in Table S1 in the supplemental material using overlap extension PCR, as described above. The final amplification product was digested with NheI and BamHI and cloned into pBBRlux linearized with SpeI and BamHI. All plasmid constructs were sequenced at the University of California, Berkeley, DNA sequencing facility to check for the fidelity of amplification.

Luminescence assays. *V. cholerae* cells harboring the plasmid indicated below were grown overnight in LB medium supplemented with chloramphenicol at 5 μg/ml. Cells were then diluted 1:500 in fresh LB medium supplemented with chloramphenicol at 5 μg/ml and harvested at exponential phase at an OD_{600} of 0.3 to 0.4. Luminescence was measured using a Victor3 multilabel counter (PerkinElmer, Waltham, MA), and *lux* expression is reported in relative luminescent units (RLU; counts min^{-1} ml^{-1}/OD_{600} unit). Assays were repeated with at least two biological replicates and four technical replicates.

V. cholerae cells and the isogenic Δ*hns* strain harboring the plasmid indicated below were grown on LB agar plates supplemented with chloramphenicol at 5 μg/ml for 24 h at 30°C. Colonies were scraped from the plate and resuspended in 5 ml of LB. The cell suspension was diluted to an OD_{600} of 0.3 to 0.4, and luminescence was measured as described above. Assays were repeated with five biological replicates and three technical replicates.

Generation of null mutations. An *V. cholerae* O1 El Tor A1552 rugose variant mutant with an in-frame deletion of *hns* was generated using the suicide plasmid pFY_3418 (R6K origin) according to previously published protocols (15, 40–42).

We generated a *vpsT hns* double mutant by replacing the wild-type *hns* allele with a Δ*hns*-FRT-Kan^r-FRT (where FRT is the FLP recombination target) mutated allele in a Δ*vpsT* strain using chitin-induced natural transformation as previously described (43). Briefly, the strains of interest were grown overnight in LB at 30°C with shaking The cultures were di-

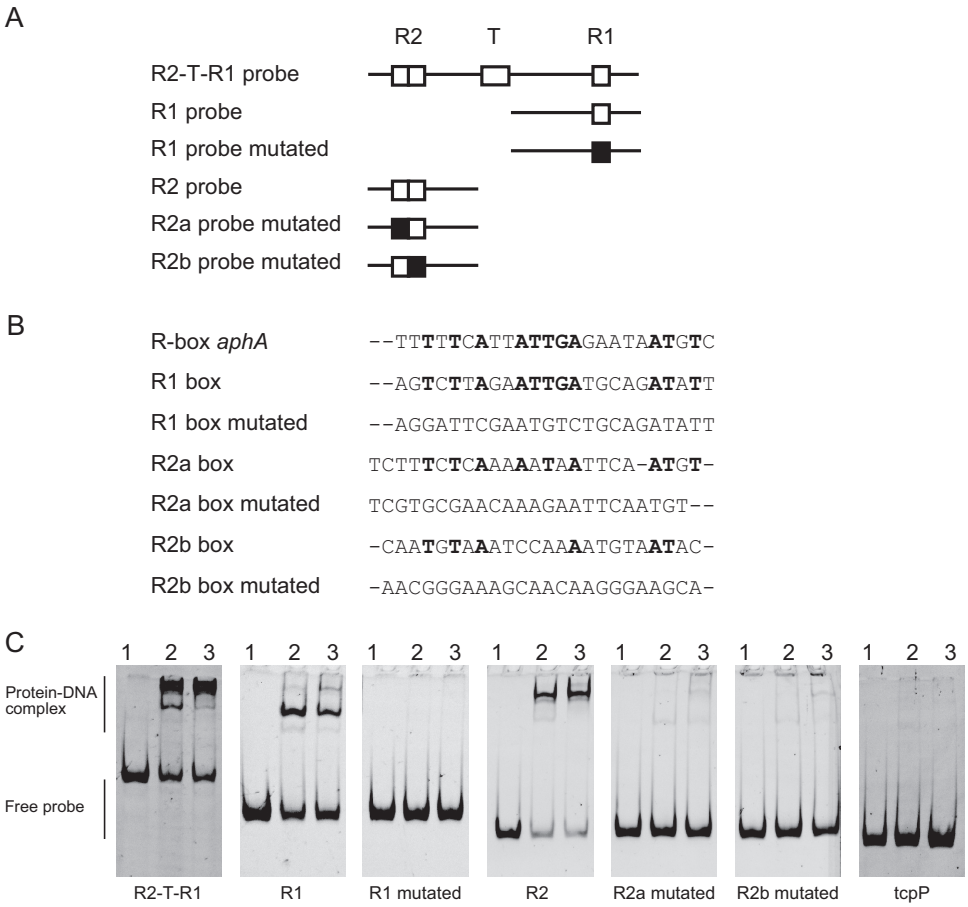

FIG 4 Analysis of the role of R1 and R2 boxes on VpsR binding. (A) Schematic representation of probes labeled with FAM used for EMSAs. The R1, R2a, R2b, and T boxes are represented as rectangles and labeled on the top. Mutated versions of the boxes used for the analysis are shown as black rectangles. (B) Alignment between the predicted R box from the *aphA* regulatory region (27, 29) and the wild-type and mutated versions of R1, R2a, and R2b. Nucleotides conserved between the predicted *aphA* R box and the R1 and R2 boxes are shown in bold. (C) Results of EMSAs performed in the presence or absence of VpsR and different probes (10 nM). Lanes 1, free probe; lanes 2, probe and 800 nM VpsR; lanes 3, probe, 800 nM VpsR, and 50 μM c-di-GMP. The probe used in every experiment is shown at the bottom of the gel.

luted 1:100 in fresh medium and grown in LB at 30°C to an OD_{600} of 0.3 to 0.5. Then, 3 ml of culture was harvested at 4,000 × *g*, washed, and resuspended in 1 ml of DASW medium (44). The suspension was added to ~50 mg of sterile chitin flakes (derived from shrimp shells [Sigma, St. Louis, MO]), and the mixture was incubated at 30°C statically overnight. The donor DNA (Δ*hns*-FRT-Kan^r-FRT) was prepared by overlapping PCR with the primers indicated in Table S1 in the supplemental material. The donor DNA (~200 ng) was resuspended in 600 μl of DASW medium, and that suspension was used to replace 600 μl of DASW medium from the cell suspension with the chitin flakes. Competent *V. cholerae* cells were incubated with the donor DNA overnight under static conditions at 30°C, and then the cells were plated on LB agar plates supplemented with kanamycin at 50 μg/ml. The insertion of the kanamycin resistance cassette at the desired location was verified by PCR.

Colony morphology and pellicle formation analysis. For colony morphology evaluation, strains were streaked on LB agar plates and grown at 30°C for 4 days. Analysis of pellicle formation was carried out with diluted (1:200) overnight cultures in glass culture tubes (18 by 150 mm) containing 5 ml of LB medium. The tubes were incubated at 30°C without shaking for 4 days. Assays were repeated with at least three different biological replicates.

Transcription factor-binding motifs. Putative binding motifs for VpsT and VpsR were inferred with the MEME (multiple expectation maximization for motif elicitation) program from a set of promoter regions of genes known to be involved in biofilm formation and identified to be significantly up- or downregulated in *vpsT* and *vpsR* mutants (VC0665, VC0916, VC0917, VC0928, VC0929, VC0930, VC0931, VC0932, VC0934, VCA0952, VC1888, VC2647, VC0583, VCA0075, and VCA0785). MEME was run to identify palindromic motifs between 10 and 30 bp long; otherwise, the default options were used. The significance of the resulting motifs was assessed by performing 10 independent runs of MEME on shuffled promoter sequences.

Computational search. Promoter regions for genes of interest were downloaded from the NCBI GenBank database and analyzed using a collection of custom Python scripts based on the Biopython library suite and available through GitHub (45). For each gene, the script downloaded the region spanning from bp +50 to −350 relative to the annotated translational start site or up to the start/end of the preceding coding region (if it was further than 350 bp upstream). Putative transcription factor-binding sites were identified using the PSSM search module of Biopython. The significance threshold for binding sites in the context of multiple-hypothesis testing was defined by computing the exact probability distributions for site scores under the PSSM and genomic background models with dynamic programming and controlling the rate of false-positive results by defining the probability of finding at least one false-positive result in a sequence of 350 bp ($\alpha_{350} = 0.01$) (46, 47).

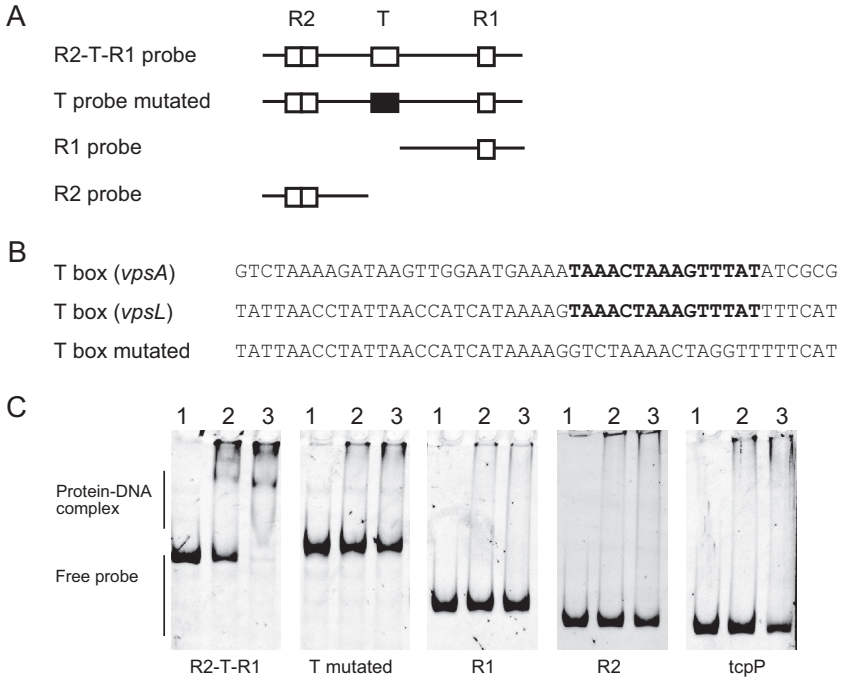

FIG 5 Analysis of the role of the T box on VpsT binding. (A) Schematic representation of probes labeled with FAM used for the EMSAs. The R1, R2a, R2b, and T boxes are represented as rectangles and labeled on the top. The mutated version of the T box is indicated by a black rectangle. (B) Alignment between T boxes from *vpsL* and *vpsA*. The palindromic region present at the core of the T box is shown in bold. (C) Results of EMSAs performed in the presence or absence of VpsT and different probes (10 nM). Lanes 1, free probe; lanes 2, probe and 300 nM VpsT; lanes 3, probe, 300 nM VpsT, and 50 μM c-di-GMP. The probe used in every experiment is shown at the bottom of the gel.

Comparative genomics analysis. The promoter sequences of *V. cholerae* O1 El Tor strain N16961 genes involved in biofilm formation (VC0665, VC0916, VC0917, VC0928, VC0929, VC0930, VC0931, VC0932, VC0934, VCA0952, VC1888, VC2647, VC0583, VCA0075, and VCA0785) were used to search all available fully sequenced and whole-genome shotgun assemblies of *V. cholerae* isolates for homologs by use of the BLASTN program (48). A list of 104 genomic assemblies containing conserved homologs for all the promoter regions of interest (those with a BLAST E value of less than 10^{-50} and more than 90% sequence identity in the BLAST alignment) was compiled and used as a reference for analyzing the promoter architecture (see Table S2 in the supplemental material). For each gene of interest, a multiple-sequence alignment of its promoter region was generated using the CLUSTALW program (49) with default parameters, and the entropy of each alignment column was computed (50). *In silico* searches for putative VpsR and VpsT binding sites were performed on all the unaligned sequences and mapped back to the multiple-sequence alignment.

RESULTS AND DISCUSSION

Determination of TSS of *vpsL*. To characterize the promoter region of *vpsL*, we first determined the transcriptional start site (TSS) of the *vpsL* gene using primer extension. RNA was isolated from the parental *V. cholerae* A1552 rugose strain harboring a *vpsL-lux* reporter (FY_Vc_9543) and as a control a Δ*vpsR* strain harboring a *vpsL-lux* reporter (FY_Vc_9544) (Table 1). The fluorescently labeled primer MSACE_*vpsL*_Rv2FAM (Fig. 1A; see also Table S1 in the supplemental material) was used for primer extension analysis. Several VpsR-dependent transcripts were identified upstream of *vpsL* (Fig. 1B and C). A comprehensive analysis of the promoter elements in *V. cholerae* has not been performed. Thus, we utilized −35 and −10 matrices from *E. coli* combined with an energy model for the spacer to identify the most conserved −10 and −35 elements of the *vpsL* regulatory region (51). The TSS of an abundant transcript was mapped to a T residue located 9 nucleotides downstream of a highly conserved −10 box of a putative σ^{70}-dependent promoter 27 bp upstream of a conserved Shine-Dalgarno sequence and 38 bp upstream of the start codon. We defined this to be the main TSS of *vpsL* based on its location with respect to the locations of the conserved −10 and −35 promoter elements (Fig. 1A). It is possible that different promoters are used to control *vpsL* expression; however, the significance of having multiple start sites for regulation of biofilm formation has yet to be determined.

Identification of VpsR and VpsT binding sites in the regulatory region of *vpsL*. To further characterize the regulatory region of *vpsL*, we determined the regions that VpsR and VpsT recognize. We conducted DNase I footprinting analysis by automated capillary electrophoresis (DFACE) using a fluorescently labeled fragment of the regulatory region of *vpsL* (positions −511 to +11 with respect to the *vpsL* translational start site) and purified recombinant MBP-VpsR and MBP-VpsT proteins. Our results revealed that VpsR is able to protect two sites (the R1 box and R2 box) separated from each other by 244 bp (Fig. 1A and 2A). The R1 box is 22 bp long (AGTCTTAGAATTGATGCAGATA) and is centered 62 bp upstream of the TSS of *vpsL*, and it matches the VpsR binding site predicted *in silico* (27). The R2 box is 40 bp long and is centered 336 bp upstream of the TSS. VpsR showed stronger protection of the R2 box than the R1 box (Fig. 2). Interestingly, the sequence of this protected region in the positive strand does not resemble that of the conserved R1 box (27). After visual inspection

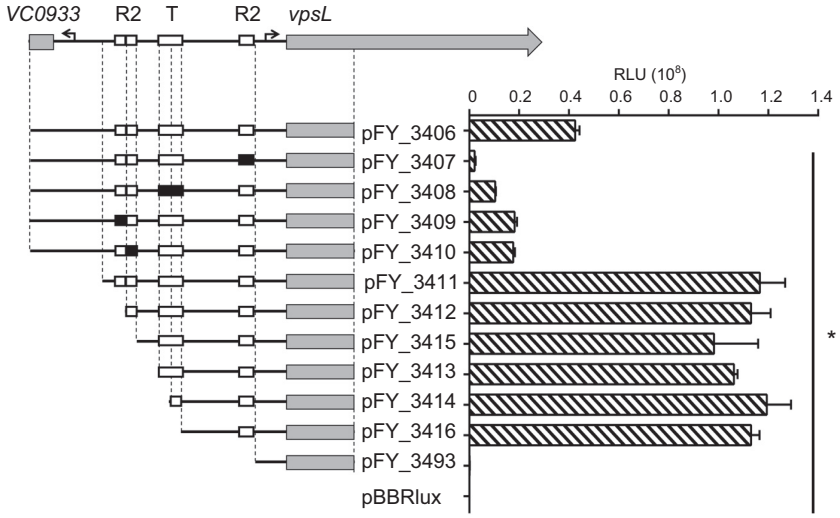

FIG 6 Analysis of the role of the R and T boxes in *vpsL* expression. A schematic representation of the regulatory region of *vpsL* that was fused to a promoterless *lux* operon is shown at the top. R boxes and T boxes are shown as empty rectangles. Mutated versions of R and T boxes are indicated by filled rectangles. Serial deletions covering the regulatory region of *vpsL* are shown at the left. The graph on the right shows the numbers of RLU obtained from the corresponding transcriptional fusions during exponential growth at 30°C. The data represent the average and standard deviation from four technical replicates from two independent biological samples. One-way analysis of variance and Dunnett's multiple-comparison test were used to determine statistically significant differences between pFY_3406 and the mutated or truncated fragments. *, $P < 0.05$.

of the complementary strand, we identified two subsites within the R2 box (R2a and R2b) that resemble the R1 motif (GAATTA TTTTTGAGAA and GTATTACATTTTGGATTTACA for R2a and R2b, respectively, where the underlined nucleotides are conserved in the R1 box). DFACE in the presence of VpsR revealed, besides the R boxes, several sites of hypersensitivity. Hypersensitivity to DNase I treatment is usually associated with DNA bending. This observation suggests that binding of VpsR might induce DNA bending at the regulatory region of *vpsL*. VpsR is structurally related to members of the NtrC family of response regulators and enhancer binding proteins (EBPs) that activate transcription at σ^{54}-dependent promoters via a process that involves DNA bending (52, 53). While several elements of the AAA-positive ATPase domain are conserved, the crucial GAFTGA motif involved in the σ^{54} interaction is missing in VpsR. Furthermore, the main targets of VpsR are not known to have σ^{54}-dependent promoters. Thus, mechanisms by which VpsR could introduce a bend upon binding to the *vpsL* regulatory region have yet to be determined.

The VpsT binding site (the T box) is 47 bp long, contains a palindromic sequence (TAAACTAAAGTTTA), and is centered 235 bp from the TSS. Thus, the location of the VpsT binding site is a considerable distance from the identified promoter elements (Fig. 1A and 3). A strong hypersensitive peak was also identified within the T box, suggesting that DNA bending could occur upon VpsT binding (Fig. 3).

The VpsT recognition sequence identified in this study is different from the one identified in the regulatory region of *rpoS* (AAAGGTTGTAAATC) (30). Thus, it appears that the VpsT recognition sequence can vary substantially. It has yet to be determined if the affinity of VpsT for these two binding motifs is different and if the strength of the interaction could be modulated by the presence of other transcriptional regulators.

Effect of mutations in the R and T boxes on VpsR and VpsT binding. To further study the role of the identified target sequences, we determined the ability of purified MBP-VpsR and MBP-VpsT to bind wild-type and mutated versions of the R box and T box, respectively, using EMSAs. To mutate the R1 and R2 boxes, nucleotides that showed strong protection in the DNase I footprint experiments and were conserved in other VpsR targets were selected (Fig. 2B and C and 4B), and transversion mutations were introduced.

Purified VpsR is able to bind to the wild-type R1 box in EMSA. However, it is unable to recognize the mutated version of the R1 box (Fig. 4C). VpsR was also able to recognize the wild-type R2 box in EMSAs, but mutations in subsites R2a and R2b abolished the ability of VpsR to bind to the R2 box, suggesting that sequence integrity of both subsites is required for binding to this region (Fig. 4C). The presence of c-di-GMP does not affect target recog-

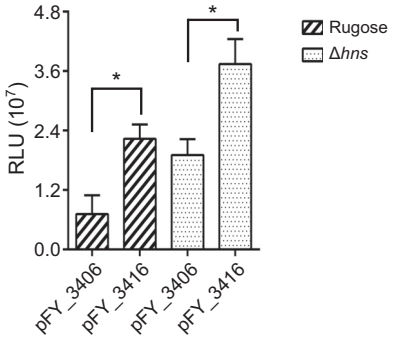

FIG 7 Analysis of expression of a shortened *vpsL* regulatory fragment in a Δ*hns* strain. Expression of P_{vpsL}-*luxCADBE* (pFY_3406) and a shortened version that starts at bp −250 upstream of the *vpsL* translational start site (pFY_3416) in a rugose strain and in a Δ*hns* strain was measured using colonies that formed after 24 h of growth at 30°C. The graph presents the average number of RLU and standard deviation obtained from four technical replicates from three independent biological samples. A two-tailed unpaired *t* test was used to compare the expression between pFY_3406 and pFY_3416 in the rugose parental strain or Δ*hns* genetic background. *, $P < 0.05$.

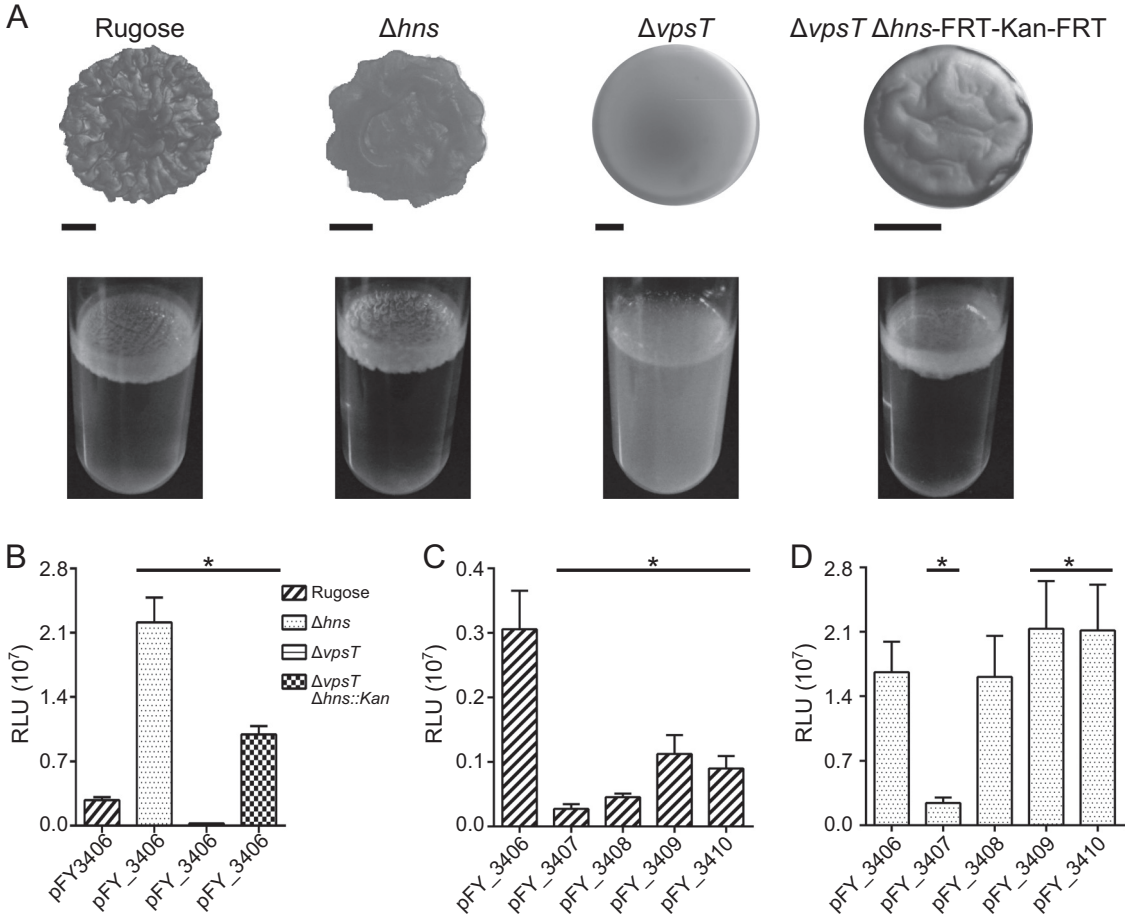

FIG 8 Analysis of biofilm formation and *vpsL* expression in Δ*hns*, Δ*vpsT*, and Δ*vpsT* Δ*hns*-FRT-Kan^r-FRT strains. (A) Colony morphology (top) and pellicle formation (bottom) of rugose and Δ*hns*, Δ*vpsT*, and Δ*vpsT* Δ*hns*-FRT-Kan^r-FRT mutant strains. Bars, 1 mm. (B) Comparison of *vpsL* expression in rugose, Δ*hns*, Δ*vpsT*, and Δ*vpsT* Δ*hns*-FRT-Kan^r-FRT strains. Expression of P_{vpsL}-*luxCADBE* was measured using colonies formed after 24 h of growth at 30°C. (C, D) Expression of P_{vpsL}-*luxCADBE* (pFY_3406) and transcriptional fusions with mutations in the R1 box (pFY_3407), T box (pFY_3408), or R2 box (pFY_3409 and pFY_3410) in rugose (C) or in an isogenic Δ*hns* strain (D) was measured using colonies formed after 24 h of growth at 30°C. The graphs present the average number of RLU and standard deviation obtained from at least three technical replicates from three to five independent biological samples. One-way analysis of variance and Dunnett's multiple-comparison test were used to determine statistically significant differences between the samples. *, $P < 0.05$.

nition by VpsR (Fig. 4C, lane 3 of each panel), in agreement with previous reports showing that c-di-GMP does not affect VpsR binding activity *in vitro* (26). Also, as a control, we showed that *in vitro* VpsR does not bind to the regulatory region of *tcpP*, a gene that does not belong to the VpsR regulon, demonstrating that the observed interaction within the regulatory region of *vpsL* is specific. These results further support the role of the R1 and R2 boxes as the binding sites for VpsR.

There is a palindromic sequence within the T box located in the upstream regulatory region of *vpsL*, and this sequence is also conserved in the regulatory region of *vpsA* (Fig. 5B). We generated transversion mutations to disrupt the palindrome and determined the ability of VpsT to recognize the mutated T-box sequence. Figure 5 shows that the palindrome at the core of the T box is essential for VpsT binding since mutations to key nucleotides disrupted binding (Fig. 5B and C). Furthermore, probes that contained only the R1 or R2 box were not recognized by VpsT. In agreement with previous reports, c-di-GMP significantly enhanced the ability of VpsT to interact with its target sequence (Fig. 5C). As in the case with VpsR, VpsT did not interact *in vitro* with the regulatory region of *tcpP*, indicating that binding to the regulatory region of *vpsL* is specific. It is important to note that VpsT forms oligomers in the presence of c-di-GMP (25). The presence of less unbound probe in the presence of VpsT and c-di-GMP (Fig. 5C) is likely to result from VpsT oligomerization and retention of DNA-protein complexes in the well.

Characterization of role of R and T boxes in control of *vpsL* expression. To evaluate the role of the R and T boxes in *vpsL* expression, we first constructed a transcriptional fusion of the regulatory region of *vpsL* (positions −607 to +158) to the promoterless *lux* operon *luxCDABE* (P_{vpsL}-*lux*). We introduced the mutations in the R1, R2, and T boxes described in the preceding section into the P_{vpsL}-*lux* upstream regulatory region. Mutations in each of these regulatory boxes negatively affected expression of *vpsL* during exponential growth at 30°C in LB, although to different extents (the order of relevance for *vpsL* expression was as follows: R1 box > T box > R_{2a} box = R_{2b} box) (Fig. 6). This finding indicates that binding of both VpsR and VpsT to their target sequences is necessary to achieve wild-type levels of *vpsL* expression. We also analyzed the ability of truncated fragments of

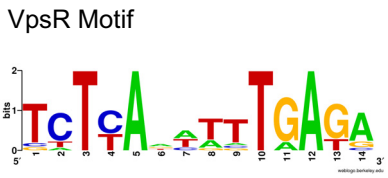

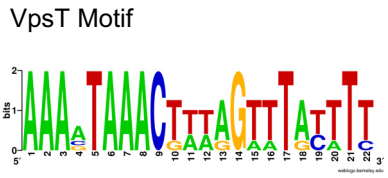

Identified sites

VC0930 (*rbmC*)	TCTCAACTTTGAGA
VC0929 (*rbmB*)	TCTCAAAGTTGAGA
VCA0952 (*vpsT*)	TCTTAATATTGAGA
VCA0075	TCTCATTTTTGAGC
VC0916 (*vpsU*)	GCTCAATTATGAGA
VC0928 (*rbmA*)	TCTTAGATTTGATA
VCA0785 (*cdgC*)	TTTTAGATTTGAGA
VC2647 (*aphA*)	TTTCATTATTGAGA
VC0665 (*vpsR*)	TCTTATCTGTGAGA
VC0934 (*vpsL*)	TCTTAGAATTGATG
VC0932 (*rbmE*)	CATCAATTCTAAGA
VC1888 (*bap1*)	TCTCACATTTAATG

Identified sites

VC0934 (*vpsL*)	AAAGTAAACTAAAGTTTATTTT
VC0932 (*rbmE*)	AAAATAAACTTTAGTTTACTTT
VC0928 (*rbmA*)	AAAATAAACTTTGGTTTATTTT
VC0917 (*vpsA*)	AAAATAAACTAAAGTTTATATC
VCA0952 (*vpsT*)	AAACTAAACGTTAGAATGCTTT

FIG 9 VpsR and VpsT motifs inferred by MEME. Top-scoring VpsR and VpsT motifs inferred by MEME on selected promoters known to be involved in biofilm formation are shown.

the *vpsL* regulatory region to activate transcription from P_{vpsL}-*lux* (Table 1 and Fig. 6). Expression of these truncated versions was elevated compared with that of the full-length P_{vpsL}-*lux* fusion in pFY_3406 (Fig. 6). It is important to note that shortened variants that lack the R2 box, the T box, or both were still highly expressed, while the absence of the R1 box abrogated *vpsL* expression. From this observation we hypothesized that the truncated P_{vpsL}-*lux* fusions are missing key structural determinants for binding of a repressor and that the R2 and T boxes participate in antirepression. It is also possible that in the shortened versions the DNA topology changes in a way that does not require binding of VpsT and VpsR to the distal boxes.

Analysis of the contribution of H-NS to *vpsL* expression. It has previously been shown that the nucleoid-binding protein H-NS can repress *vpsL* expression by directly binding to its regulatory region (32). The exact coverage of H-NS at the *vpsL* promoter has not been reported. Nonetheless, it has been shown that this regulator can oligomerize and bind to AT-rich sequences to silence transcription (54, 55). We asked whether the increase in expression of the reporter construct lacking the R2 and T boxes was due to the loss of repression by H-NS. Thus, we compared the expression of a full-length fragment (pFY_3406) and a fragment lacking the R2 and T boxes (pFY_3416) in a rugose strain and an isogenic Δ*hns* strain (Fig. 7). Our results revealed, in agreement with the findings presented in a previous report (32), that in the Δ*hns* strain the expression of *vpsL* was increased (pFY_3406) compared to that of rugose. The levels of expression of the pFY_3406 construct in the Δ*hns* strain were similar to the levels of expression of pFY_3416 in the rugose strain. However, in the Δ*hns* strain the expression of pFY_3416 was higher than that of pFY_3406. Collectively, these finding suggest that, in addition to the absence of HN-S, other regulatory factors contribute to increased *vpsL* expression in the reporter construct lacking the R2 and T boxes.

Genetic interaction analysis of *hns* and *vpsT*. The silencing activity of H-NS at the regulatory region of the *ctx* and *tcpA* genes can be counteracted by a major virulence regulator, ToxT (55). To analyze if VpsT can act in a similar way at the *vpsL* regulatory region, we characterized the genetic interaction between *vpsT* and *hns*. For this purpose we generated a *vpsT* and *hns* double mutation (Δ*vpsT* Δ*hns*-FRT-Kan^r-FRT) in the *V. cholerae* A1552 rugose strain.

We first compared the biofilm formation of the rugose strain, the single Δ*hns* and Δ*vpsT* mutants, and the *vpsT* and *hns* double mutant. The deletion of *hns* resulted in an increase in colony compactness (which is typically associated with enhanced biofilm matrix production) and pellicle corrugation (Fig. 8A), corroborating previous work showing that strains lacking H-NS exhibit enhanced biofilm formation (32). The Δ*vpsT* strain had a smooth colony morphology and lost its ability to form pellicles. The Δ*vpsT* Δ*hns* mutant exhibited a decrease in the level of both colony and pellicle corrugation compared to that of the parental rugose strain (Fig. 8). This finding suggests that the presence of VpsT is necessary to produce biofilm matrix at the parental level, even in the absence of the repressor H-NS. Furthermore, we compared the expression of *vpsL* from pFY_3406 in the rugose parental strain and the Δ*hns*, Δ*vpsT*, and Δ*vpsT* Δ*hns* mutants (Fig. 8B). As previously reported, we found that the expression of *vpsL* was increased in the absence of H-NS and decreased in the absence of VpsT (24, 32). In the Δ*vpsT* Δ*hns* mutant, *vpsL* was expressed at levels higher than those observed in the parental rugose strain and the Δ*vpsT* strain. However, the expression of *vpsL* in the Δ*hns* Δ*vpsT* mutant was not as high as that in the Δ*hns* mutant. This finding suggests that in the absence of *vpsT*, expression of *vpsL* can be activated to levels even higher than those in the parental strain, provided that the H-NS repressor is also absent. Nonetheless, VpsT is still necessary to achieve the highest levels of expression of *vpsL* observed in a Δ*hns* mutant.

Since VpsT can promote *vpsL* expression both directly by binding to the *vpsL* promoter region and indirectly through the modulation of *vpsR* expression, we then evaluated if direct binding of VpsT to the *vpsL* promoter region was necessary to promote expression in the absence of H-NS. We compared the expression of *vpsL* from pFY_3406, pFY_3407, pFY_3408, pFY_3409, and pFY_3410 (containing wild-type and mutated versions of the R1,

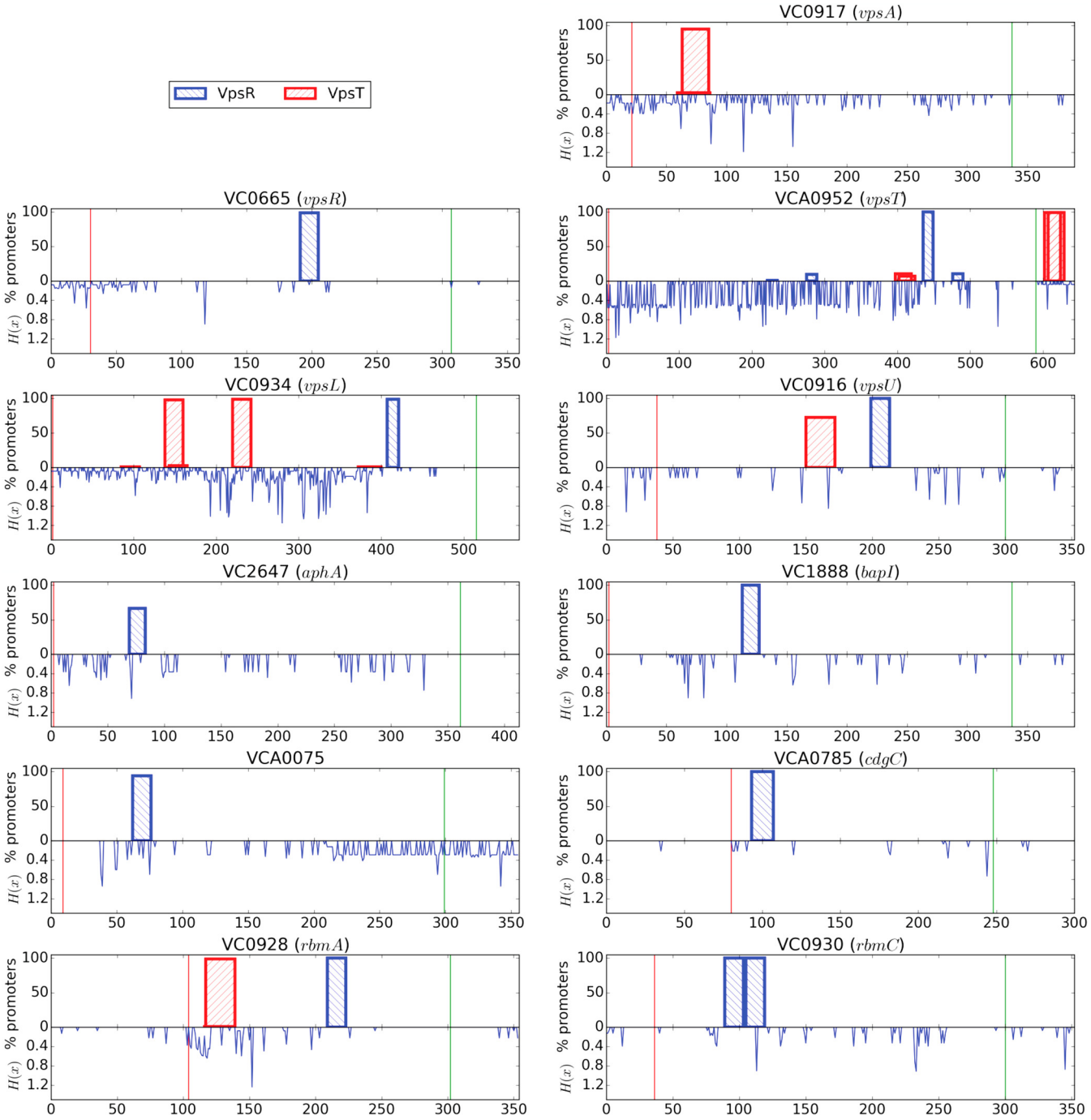

FIG 10 Cross regulation and conservation analysis for promoters of genes involved in biofilm formation. For each gene, patterned boxes on the upper *y* axis represent the percentage of homologous promoter sequences that contain a predicted functional binding site (those with a score above the significance threshold) for VpsR and VpsT. The lower *y* axis shows the positional entropy [$H(x)$] of the multiple-sequence alignment for each set of homologous promoters. Higher entropy values correspond to lower levels of sequence conservation. Green line, the predicted translational start site for each gene; red line, the predicted translational start/end for the first gene upstream. *x*-axis values are in base pairs.

T, and R2 boxes) in the rugose strain and the Δ*hns* mutant (Fig. 8B and C). In the rugose strain, mutations in the R1, T, and R2 boxes decreased the level of expression of *vpsL* (Fig. 7B). In a Δ*hns* mutant, mutations in the R1 box decreased the level of expression of *vpsL*, while mutations in the T box did not, and mutations in the R2 box resulted in a modest increase in the level of *vpsL* expression (Fig. 7C). These results led us to propose that in the absence of H-NS, direct binding of VpsT is not necessary to promote expression of *vpsL*.

Collectively, these results suggest that VpsT plays a role in counteracting the silencing activity of H-NS at the regulatory region of *vpsL* but that it also regulates biofilm formation indepen-

dently from H-NS. Additionally, we show that VpsR interacts at two sites in the regulatory region of *vpsL*: the distal binding site seems to play a role similar to that of the T box, interfering with H-NS activity, while the proximal R1 box seems to be crucial for direct activation. This evidence supports a regulatory model where VpsR acts as both an antirepressor and a direct activator of *vpsL*, while VpsT is mainly required to overcome, to a certain extent, the silencing effect exerted by H-NS. As mentioned above, antisilencing plays a role in the control of *ctx* and *tcpA* expression, with ToxT acting as both an antirepressor and a direct activator of gene expression (55). Our results suggest that a similar regulatory mechanism could be operating in the regulatory region of *vpsL*, but in this case, two positive regulators would be involved.

***In silico* analysis of VpsT and VpsR regulation of genes involved in biofilm formation.** To further elucidate the combined role of VpsR and VpsT in the regulation of biofilm formation, we performed a detailed *in silico* analysis of the promoter regions of genes associated with biofilm formation (Fig. 9). VpsT and VpsR binding motifs on the upstream sequences of genes that are known to be involved in biofilm formation and whose expression exhibits strong dependence on VpsR and VpsT were inferred using MEME (multiple EM for motif elicitation) (14, 15, 19, 24, 27, 29, 56, 57) (Fig. 9). The two top-scoring palindromic motifs inferred by MEME mapped to the previously established binding motif for VpsR (26, 27) and to the core sequence elements of the *vpsL* R and T boxes identified in this work, supporting the notion that these motifs define the essential binding determinants for VpsT and VpsR across multiple target promoters.

To obtain a more comprehensive picture of the role of VpsR and VpsT in the regulation of biofilm formation in *V. cholerae*, we analyzed the conservation profiles of predicted VpsR and VpsT binding sites on *V. cholerae* promoters linked to biofilm formation across 104 *V. cholerae* isolates (Fig. 10). This *in silico* analysis revealed that some of the biofilm genes might be independently activated by VpsR or VpsT. The *vpsA* gene can be expressed from the *vpsU* promoter and by an additional promoter located in the intergenic region between *vpsA* and *vpsU*. A conserved R box was not found in this intergenic region; however, a highly conserved T box was present. Upstream regulatory regions of the genes encoding biofilm matrix proteins, c-di-GMP metabolic enzymes, and regulators involved in biofilm formation, including *bap1*, *rbmC*, *cdgA*, *cdgC*, and *aphA*, are predicted to be directly regulated by VpsR but not by VpsT (Fig. 10).

Overall, predicted sites for both regulators appear to be conserved across the analyzed *V. cholerae* isolates and tend to be associated with regions of higher conservation within promoter regions, suggesting that purifying selection is preserving functional sites. Conservation patterns across promoters, however, vary significantly. The promoters of the *vpsR* and *cdgC* genes show the least amount of variability, whereas the *vpsA*, *vpsL*, and *vpsT* promoters evidence a significant amount of polymorphism. Furthermore, the apparent loss of VpsT regulation for the *vpsU* promoter in some strains, as well as the prediction of novel functional sites for VpsR and VpsT on the *vpsT* promoter, suggests that regulation of biofilm matrix formation is under active selection among extant *V. cholerae* strains.

Based on this *in silico* analysis, we propose that VpsR and VpsT directly coregulate the expression of the *vps* operons, certain *rbm* genes, and *vpsT* by binding simultaneously or independently (Fig. 10). This observation suggests that the combined regulatory activity of VpsR and VpsT on these target promoters is a necessary component for the full induction of the biofilm formation pathway, even though the specific mechanism of action at each promoter may differ.

ACKNOWLEDGMENTS

This work was supported by NIH grant R01AI055987 (to F.H.Y.) and by U.S. National Science Foundation grant MCB-1158056 (to I.E.). D.Z.-S. was supported by a UC-MEXUS fellowship.

We thank Jennifer Teschler and Jenna Conner for their comments on the manuscript.

REFERENCES

1. **Flemming H-C, Wingender J.** 2010. The biofilm matrix. Nat Rev Microbiol **8:**623–633. http://dx.doi.org/10.1038/nrmicro2415.
2. **Charles RC, Ryan ET.** 2011. Cholera in the 21st century. Curr Opin Infect Dis **24:**472–477. http://dx.doi.org/10.1097/QCO.0b013e32834a88af.
3. **Faruque SM, Albert MJ, Mekalanos JJ.** 1998. Epidemiology, genetics, and ecology of toxigenic *Vibrio cholerae*. Microbiol Mol Biol Rev **62:**1301–1314.
4. **Huq A, Colwell RR, Chowdhury MA, Xu B, Moniruzzaman SM, Islam MS, Yunus M, Albert MJ.** 1995. Coexistence of *Vibrio cholerae* O1 and O139 Bengal in plankton in Bangladesh. Lancet **345:**1249. http://dx.doi.org/10.1016/S0140-6736(95)92038-2.
5. **Islam MS, Jahid MIK, Rahman MM, Rahman MZ, Islam MS, Kabir MS, Sack DA, Schoolnik GK.** 2007. Biofilm acts as a microenvironment for plankton-associated *Vibrio cholerae* in the aquatic environment of Bangladesh. Microbiol Immunol **51:**369–379. http://dx.doi.org/10.1111/j.1348-0421.2007.tb03924.x.
6. **Hood M, Winter P.** 2006. Attachment of *Vibrio cholerae* under various environmental conditions and to selected substrates. FEMS Microbiol Ecol **22:**215–223. http://dx.doi.org/10.1111/j.1574-6941.1997.tb00373.x.
7. **Huq A, Small EB, West PA, Huq MI, Rahman R, Colwell RR.** 1983. Ecological relationships between *Vibrio cholerae* and planktonic crustacean copepods. Appl Environ Microbiol **45:**275–283.
8. **Huq A, West PA, Small EB, Huq MI, Colwell RR.** 1984. Influence of water temperature, salinity, and pH on survival and growth of toxigenic *Vibrio cholerae* serovar O1 associated with live copepods in laboratory microcosms. Appl Environ Microbiol **48:**420–424.
9. **Alam M, Sultana M, Nair GB, Siddique AK, Hasan NA, Sack RB, Sack DA, Ahmed KU, Sadique A, Watanabe H, Grim CJ, Huq A, Colwell RR.** 2007. Viable but nonculturable *Vibrio cholerae* O1 in biofilms in the aquatic environment and their role in cholera transmission. Proc Natl Acad Sci U S A **104:**17801–17806. http://dx.doi.org/10.1073/pnas.0705599104.
10. **Colwell RR, Huq A, Islam MS, Aziz KMA, Yunus M, Khan NH, Mahmud A, Sack RB, Nair GB, Chakraborty J, Sack DA, Russek-Cohen E.** 2003. Reduction of cholera in Bangladeshi villages by simple filtration. Proc Natl Acad Sci U S A **100:**1051–1055. http://dx.doi.org/10.1073/pnas.0237386100.
11. **Faruque SM, Biswas K, Udden SMN, Ahmad QS, Sack DA, Nair GB, Mekalanos JJ.** 2006. Transmissibility of cholera: in vivo-formed biofilms and their relationship to infectivity and persistence in the environment. Proc Natl Acad Sci U S A **103:**6350–6355. http://dx.doi.org/10.1073/pnas.0601277103.
12. **Yildiz FH, Schoolnik GK.** 1999. *Vibrio cholerae* O1 El Tor: identification of a gene cluster required for the rugose colony type, exopolysaccharide production, chlorine resistance, and biofilm formation. Proc Natl Acad Sci U S A **96:**4028–4033. http://dx.doi.org/10.1073/pnas.96.7.4028.
13. **Yildiz F, Fong J, Sadovskaya I, Grard T, Vinogradov E.** 2014. Structural characterization of the extracellular polysaccharide from *Vibrio cholerae* O1 El-Tor. PLoS One **9:**e86751. http://dx.doi.org/10.1371/journal.pone.0086751.
14. **Fong JCN, Karplus K, Schoolnik GK, Yildiz FH.** 2006. Identification and characterization of RbmA, a novel protein required for the development of rugose colony morphology and biofilm structure in *Vibrio cholerae*. J Bacteriol **188:**1049–1059. http://dx.doi.org/10.1128/JB.188.3.1049-1059.2006.
15. **Fong JCN, Yildiz FH.** 2007. The *rbmBCDEF* gene cluster modulates development of rugose colony morphology and biofilm formation in

Vibrio cholerae. J Bacteriol **189:**2319–2330. http://dx.doi.org/10.1128/JB.01569-06.
16. **Moorthy S, Watnick PI.** 2005. Identification of novel stage-specific genetic requirements through whole genome transcription profiling of *Vibrio cholerae* biofilm development. Mol Microbiol **57:**1623–1635. http://dx.doi.org/10.1111/j.1365-2958.2005.04797.x.
17. **Absalon C, Van Dellen K, Watnick PI.** 2011. A communal bacterial adhesin anchors biofilm and bystander cells to surfaces. PLoS Pathog **7:**e1002210. http://dx.doi.org/10.1371/journal.ppat.1002210.
18. **Berk V, Fong JCN, Dempsey GT, Develioglu ON, Zhuang X, Liphardt J, Yildiz FH, Chu S.** 2012. Molecular architecture and assembly principles of *Vibrio cholerae* biofilms. Science **337:**236–239. http://dx.doi.org/10.1126/science.1222981.
19. **Fong JCN, Syed KA, Klose KE, Yildiz FH.** 2010. Role of *Vibrio* polysaccharide (*vps*) genes in VPS production, biofilm formation and *Vibrio cholerae* pathogenesis. Microbiology **156:**2757–2769. http://dx.doi.org/10.1099/mic.0.040196-0.
20. **Tischler AD, Camilli A.** 2004. Cyclic diguanylate (c-di-GMP) regulates *Vibrio cholerae* biofilm formation. Mol Microbiol **53:**857–869. http://dx.doi.org/10.1111/j.1365-2958.2004.04155.x.
21. **Beyhan S, Tischler AD, Camilli A, Yildiz FH.** 2006. Transcriptome and phenotypic responses of *Vibrio cholerae* to increased cyclic di-GMP level. J Bacteriol **188:**3600–3613. http://dx.doi.org/10.1128/JB.188.10.3600-3613.2006.
22. **Beyhan S, Yildiz FH.** 2007. Smooth to rugose phase variation in *Vibrio cholerae* can be mediated by a single nucleotide change that targets c-di-GMP signalling pathway. Mol Microbiol **63:**995–1007. http://dx.doi.org/10.1111/j.1365-2958.2006.05568.x.
23. **Yildiz FH, Dolganov NA, Schoolnik GK.** 2001. VpsR, a member of the response regulators of the two-component regulatory systems, is required for expression of *vps* biosynthesis genes and EPS(ETr)-associated phenotypes in *Vibrio cholerae* O1 El Tor. J Bacteriol **183:**1716–1726. http://dx.doi.org/10.1128/JB.183.5.1716-1726.2001.
24. **Casper-Lindley C, Yildiz FH.** 2004. VpsT is a transcriptional regulator required for expression of *vps* biosynthesis genes and the development of rugose colonial morphology in *Vibrio cholerae* O1 El Tor. J Bacteriol **186:**1574–1578. http://dx.doi.org/10.1128/JB.186.5.1574-1578.2004.
25. **Krasteva PV, Fong JCN, Shikuma NJ, Beyhan S, Navarro MVAS, Yildiz FH, Sondermann H.** 2010. *Vibrio cholerae* VpsT regulates matrix production and motility by directly sensing cyclic di-GMP. Science **327:**866–868. http://dx.doi.org/10.1126/science.1181185.
26. **Srivastava D, Harris RC, Waters CM.** 2011. Integration of cyclic di-GMP and quorum sensing in the control of *vpsT* and *aphA* in *Vibrio cholerae*. J Bacteriol **193:**6331–6341. http://dx.doi.org/10.1128/JB.05167-11.
27. **Yildiz FH, Liu XS, Heydorn A, Schoolnik GK.** 2004. Molecular analysis of rugosity in a *Vibrio cholerae* O1 El Tor phase variant. Mol Microbiol **53:**497–515. http://dx.doi.org/10.1111/j.1365-2958.2004.04154.x.
28. **Beyhan S, Bilecen K, Salama SR, Casper-Lindley C, Yildiz FH.** 2007. Regulation of rugosity and biofilm formation in *Vibrio cholerae*: comparison of VpsT and VpsR regulons and epistasis analysis of *vpsT*, *vpsR*, and *hapR*. J Bacteriol **189:**388–402. http://dx.doi.org/10.1128/JB.00981-06.
29. **Lin W, Kovacikova G, Skorupski K.** 2007. The quorum sensing regulator HapR downregulates the expression of the virulence gene transcription factor AphA in *Vibrio cholerae* by antagonizing Lrp- and VpsR-mediated activation. Mol Microbiol **64:**953–967. http://dx.doi.org/10.1111/j.1365-2958.2007.05693.x.
30. **Wang H, Ayala JC, Benitez JA, Silva AJ.** 2014. The LuxR-type regulator VpsT negatively controls the transcription of *rpoS*, encoding the general stress response regulator, in *Vibrio cholerae* biofilms. J Bacteriol **196:**1020–1030. http://dx.doi.org/10.1128/JB.00993-13.
31. **Waters CM, Lu W, Rabinowitz JD, Bassler BL.** 2008. Quorum sensing controls biofilm formation in *Vibrio cholerae* through modulation of cyclic di-GMP levels and repression of *vpsT*. J Bacteriol **190:**2527–2536. http://dx.doi.org/10.1128/JB.01756-07.
32. **Wang H, Ayala JC, Silva AJ, Benitez JA.** 2012. The histone-like nucleoid structuring protein (H-NS) is a repressor of *Vibrio cholerae* exopolysaccharide biosynthesis (*vps*) genes. Appl Environ Microbiol **78:**2482–2488. http://dx.doi.org/10.1128/AEM.07629-11.
33. **Liang W, Silva AJ, Benitez JA.** 2007. The cyclic AMP receptor protein modulates colonial morphology in *Vibrio cholerae*. Appl Environ Microbiol **73:**7482–7487. http://dx.doi.org/10.1128/AEM.01564-07.
34. **Liang W, Pascual-Montano A, Silva AJ, Benitez JA.** 2007. The cyclic AMP receptor protein modulates quorum sensing, motility and multiple genes that affect intestinal colonization in *Vibrio cholerae*. Microbiology **153:**2964–2975. http://dx.doi.org/10.1099/mic.0.2007/006668-0.
35. **Fong JCN, Yildiz FH.** 2008. Interplay between cyclic AMP-cyclic AMP receptor protein and cyclic di-GMP signaling in *Vibrio cholerae* biofilm formation. J Bacteriol **190:**6646–6659. http://dx.doi.org/10.1128/JB.00466-08.
36. **Untergasser A, Cutcutache I, Koressaar T, Ye J, Faircloth BC, Remm M, Rozen SG.** 2012. Primer3—new capabilities and interfaces. Nucleic Acids Res **40:**e115. http://dx.doi.org/10.1093/nar/gks596.
37. **Merighi M, Majerczak DR, Zianni M, Tessanne K, Coplin DL.** 2006. Molecular characterization of *Pantoea stewartii* subsp. *stewartii* HrpY, a conserved response regulator of the Hrp type III secretion system, and its interaction with the *hrpS* promoter. J Bacteriol **188:**5089–5100. http://dx.doi.org/10.1128/JB.01929-05.
38. **Zianni M, Tessanne K, Merighi M, Laguna R, Tabita FR.** 2006. Identification of the DNA bases of a DNase I footprint by the use of dye primer sequencing on an automated capillary DNA analysis instrument. J Biomol Tech **17:**103–113.
39. **Joshi GS, Zianni M, Bobst CE, Tabita FR.** 2012. Further unraveling the regulatory twist by elucidating metabolic coinducer-mediated CbbR-*cbbI* promoter interactions in *Rhodopseudomonas palustris* CGA010. J Bacteriol **194:**1350–1360. http://dx.doi.org/10.1128/JB.06418-11.
40. **Miller VL, Mekalanos JJ.** 1988. A novel suicide vector and its use in construction of insertion mutations: osmoregulation of outer membrane proteins and virulence determinants in *Vibrio cholerae* requires *toxR*. J Bacteriol **170:**2575–2583.
41. **Fullner KJ, Mekalanos JJ.** 1999. Genetic characterization of a new type IV-A pilus gene cluster found in both classical and El Tor biotypes of *Vibrio cholerae*. Infect Immun **67:**1393–1404.
42. **Shikuma NJ, Yildiz FH.** 2009. Identification and characterization of OscR, a transcriptional regulator involved in osmolarity adaptation in *Vibrio cholerae*. J Bacteriol **191:**4082–4096. http://dx.doi.org/10.1128/JB.01540-08.
43. **De Souza Silva O, Blokesch M.** 2010. Genetic manipulation of *Vibrio cholerae* by combining natural transformation with FLP recombination. Plasmid **64:**186–195. http://dx.doi.org/10.1016/j.plasmid.2010.08.001.
44. **Meibom KL, Blokesch M, Dolganov NA, Wu C-Y, Schoolnik GK.** 2005. Chitin induces natural competence in *Vibrio cholerae*. Science **310:**1824–1827. http://dx.doi.org/10.1126/science.1120096.
45. **Cock PJA, Antao T, Chang JT, Chapman BA, Cox CJ, Dalke A, Friedberg I, Hamelryck T, Kauff F, Wilczynski B, de Hoon MJL.** 2009. Biopython: freely available Python tools for computational molecular biology and bioinformatics. Bioinformatics **25:**1422–1423. http://dx.doi.org/10.1093/bioinformatics/btp163.
46. **Rahmann S, Müller T, Vingron M.** 2003. On the power of profiles for transcription factor binding site detection. Stat Appl Genet Mol Biol **2:**Article 7. http://dx.doi.org/10.2202/1544-6115.1032.
47. **Beckstette M, Homann R, Giegerich R, Kurtz S.** 2006. Fast index based algorithms and software for matching position specific scoring matrices. BMC Bioinformatics **7:**389. http://dx.doi.org/10.1186/1471-2105-7-389.
48. **Altschul SF, Madden TL, Schäffer AA, Zhang J, Zhang Z, Miller W, Lipman DJ.** 1997. Gapped BLAST and PSI-BLAST: a new generation of protein database search programs. Nucleic Acids Res **25:**3389–3402. http://dx.doi.org/10.1093/nar/25.17.3389.
49. **Thompson JD, Higgins DG, Gibson TJ.** 1994. CLUSTAL W: improving the sensitivity of progressive multiple sequence alignment through sequence weighting, position-specific gap penalties and weight matrix choice. Nucleic Acids Res **22:**4673–4680. http://dx.doi.org/10.1093/nar/22.22.4673.
50. **Erill I, O'Neill MC.** 2009. A reexamination of information theory-based methods for DNA-binding site identification. BMC Bioinformatics **10:**57. http://dx.doi.org/10.1186/1471-2105-10-57.
51. **Klucar L, Stano M, Hajduk M.** 2010. phiSITE: database of gene regulation in bacteriophages. Nucleic Acids Res **38:**D366–D370. http://dx.doi.org/10.1093/nar/gkp911.
52. **Lilja AE, Jenssen JR, Kahn JD.** 2004. Geometric and dynamic requirements for DNA looping, wrapping and unwrapping in the activation of *E. coli glnAp2* transcription by NtrC. J Mol Biol **342:**467–478. http://dx.doi.org/10.1016/j.jmb.2004.07.057.
53. **De Carlo S, Chen B, Hoover TR, Kondrashkina E, Nogales E, Nixon BT.** 2006. The structural basis for regulated assembly and function of the transcriptional activator NtrC. Genes Dev **20:**1485–1495. http://dx.doi.org/10.1101/gad.1418306.

54. **Nye MB, Pfau JD, Skorupski K, Taylor RK.** 2000. *Vibrio cholerae* H-NS silences virulence gene expression at multiple steps in the ToxR regulatory cascade. J Bacteriol **182:**4295–4303. http://dx.doi.org/10.1128/JB.182.15.4295-4303.2000.
55. **Yu RR, DiRita VJ.** 2002. Regulation of gene expression in *Vibrio cholerae* by ToxT involves both antirepression and RNA polymerase stimulation. Mol Microbiol **43:**119–134. http://dx.doi.org/10.1046/j.1365-2958.2002.02721.x.
56. **Yang M, Frey EM, Liu Z, Bishar R, Zhu J.** 2010. The virulence transcriptional activator AphA enhances biofilm formation by *Vibrio cholerae* by activating expression of the biofilm regulator VpsT. Infect Immun **78:**697–703. http://dx.doi.org/10.1128/IAI.00429-09.
57. **Lim B, Beyhan S, Meir J, Yildiz FH.** 2006. Cyclic-diGMP signal transduction systems in *Vibrio cholerae*: modulation of rugosity and biofilm formation. Mol Microbiol **60:**331–348. http://dx.doi.org/10.1111/j.1365-2958.2006.05106.x.
58. **Herrero M, de Lorenzo V, Timmis KN.** 1990. Transposon vectors containing non-antibiotic resistance selection markers for cloning and stable chromosomal insertion of foreign genes in gram-negative bacteria. J Bacteriol **172:**6557–6567.
59. **De Lorenzo V, Timmis KN.** 1994. Analysis and construction of stable phenotypes in gram-negative bacteria with Tn5- and Tn10-derived minitransposons. Methods Enzymol **235:**386–405. http://dx.doi.org/10.1016/0076-6879(94)35157-0.
60. **Lenz DH, Mok KC, Lilley BN, Kulkarni RV, Wingreen NS, Bassler BL.** 2004. The small RNA chaperone Hfq and multiple small RNAs control quorum sensing in *Vibrio harveyi* and *Vibrio cholerae*. Cell **118:**69–82. http://dx.doi.org/10.1016/j.cell.2004.06.009.
61. **Blokesch M.** 2012. TransFLP—a method to genetically modify *Vibrio cholerae* based on natural transformation and FLP-recombination. J Vis Exp **2012:**3761. http://dx.doi.org/10.3791/3761.